

Propagation of designer surface plasmons in structured conductor surfaces with parabolic gradient index

Bala Krishna Juluri¹, Sz-Chin S. Lin¹, Thomas R. Walker¹, Lasse Jensen^{2*}
and Tony Jun Huang^{1*}

¹ Department of Engineering Science and Mechanics, The Pennsylvania State University, University Park, PA 16802, USA

² Department of Chemistry, The Pennsylvania State University, University Park, PA 16802, USA

*Corresponding authors: jensen@chem.psu.edu (L. J.) & junhuang@psu.edu (T. J. H)

Abstract: In this work, we investigate the propagation of designer surface plasmons in planar perfect electric conductor structures that are subject to a parabolic graded-index distribution. A three-dimensional, fully vectorial finite-difference time-domain method was used to engineer a structure with a parabolic effective group index by modulating the dielectric constant of the structure's square holes. Using this structure in our simulations, the lateral confinement of propagating designer surface plasmons is demonstrated. Focusing, collimation and waveguiding of designer plasmons in the lateral direction is realized by changing the width of the source beam. Our findings contribute to applications of designer surface plasmons that require energy concentration, diffusion, guiding, and beam aperture modification within planar perfect electric conductors.

© 2009 Optical Society of America

OCIS codes: (240.6680) Surface plasmons; (120.1680) Collimation; (130.2790) Guided Waves; (260.5950) Self-focusing

References and links

1. T. Ebbesen, H. Lezec, H. Ghaemi, T. Thio, and P. Wolff, "Extraordinary optical transmission through sub-wavelength hole arrays," *Nature* **391**, 667–669 (1998). URL <http://www.nature.com/nature/journal/v391/n6668/abs/391667a0.html>.
2. L. Martín-Moreno, F. J. García-Vidal, H. J. Lezec, K. M. Pellerin, T. Thio, J. B. Pendry, and T. W. Ebbesen, "Theory of Extraordinary Optical Transmission through Subwavelength Hole Arrays," *Phys. Rev. Lett.* **86**, 1114–1117 (2001). URL <http://link.aps.org/abstract/PRL/v86/p1114>.
3. J. B. Pendry, L. Martín-Moreno, and F. J. Garcia-Vidal, "Mimicking Surface Plasmons with Structured Surfaces," *Science* **305**, 847–848 (2004). URL <http://www.sciencemag.org/cgi/content/abstract/305/5685/847>.
4. F. J. Garcia-Vidal, L. Martín-Moreno, and J. B. Pendry, "Surfaces with holes in them: new plasmonic metamaterials," *J. Opt. A: Pure Appl. Opt.* **7**, S97–S101 (2005). URL <http://www.iop.org/EJ/abstract/1464-4258/7/2/013/>.
5. F. J. G. de Abajo and J. J. Sáenz, "Electromagnetic Surface Modes in Structured Perfect-Conductor Surfaces," *Phys. Rev. Lett.* **95**, 233901-1–4 (2005). URL <http://link.aps.org/abstract/PRL/v95/e233901>.
6. M. Qiu, "Photonic band structures for surface waves on structured metal surfaces," *Opt. Express* **13**, 7583–7588 (2005). URL <http://www.opticsexpress.org/abstract.cfm?uri=oe-13-19-7583>.
7. A. Hibbins, B. Evans, and J. Sambles, "Experimental Verification of Designer Surface Plasmons," *Science* **308**, 670–672 (2005). URL <http://www.sciencemag.org/cgi/content/abstract/308/5722/670>.
8. A. P. Hibbins, M. J. Lockyear, I. R. Hooper, and J. R. Sambles, "Waveguide Arrays as Plasmonic Metamaterials: Transmission below Cutoff," *Phys. Rev. Lett.* **96**, 073904-1–5 (2006). URL <http://link.aps.org/abstract/PRL/v96/e073904>.

9. C. R. Williams, S. R. Andrews, S. A. Maier, A. I. Fernández-Domínguez, L. Martín-Moreno, and F. J. García-Vidal, "Highly confined guiding of terahertz surface plasmon polaritons on structured metal surfaces," *Nat. Photonics* **2**, 175–179 (2008). URL <http://www.nature.com/nphoton/journal/v2/n3/abs/nphoton.2007.301.html>.
10. W. Zhu, A. Agrawal, and A. Nahata, "Planar plasmonic terahertz guided-wave devices," *Opt. Express* **16**, 6216–6226 (2008). URL <http://www.opticsexpress.org/abstract.cfm?URI=oe-16-9-6216>.
11. H. Cao and A. Nahata, "Resonantly enhanced transmission of terahertz radiation through a periodic array of subwavelength apertures," *Opt. Express* **12**, 1004–1010 (2004). URL <http://www.opticsinfobase.org/abstract.cfm?URI=oe-12-6-1004>.
12. F. Miyamaru and M. Hangyo, "Strong enhancement of terahertz transmission for a three-layer heterostructure of metal hole arrays," *Phys. Rev. B* **72**, 035429-1–5 (2005). URL <http://link.aps.org/abstract/PRB/v72/e035429>.
13. J. Gómez Rivas, C. Schotsch, P. Haring Bolívar, and H. Kurz, "Enhanced transmission of THz radiation through subwavelength holes," *Phys. Rev. B* **68**, 201306-1–4 (2003). URL <http://link.aps.org/abstract/PRB/v68/e201306>.
14. A. P. Hibbins, J. R. Sambles, and C. R. Lawrence, "Grating-coupled surface plasmons at microwave frequencies," *J. Appl. Phys.* **86**, 1791–1795 (1999). URL <http://link.aip.org/link/?JAP/86/1791/1>.
15. M. Johnston, "Plasmonics: Superfocusing of terahertz waves," *Nat. Photonics* **1**, 14–15 (2007). URL <http://www.nature.com/nphoton/journal/v1/n1/full/nphoton.2006.60.html>.
16. J. Gómez Rivas, "Terahertz: The art of confinement," *Nat. Photonics* **2**, 137–138 (2008). URL <http://www.nature.com/nphoton/journal/v2/n3/abs/nphoton.2008.12.html>.
17. D. Wu, N. Fang, C. Sun, X. Zhang, W. Padilla, D. Basov, D. Smith, and S. Schultz, "Terahertz plasmonic high pass filter," *Appl. Phys. Lett.* **83**, 201–203 (2003). URL <http://link.aip.org/link/?APPLAB/83/201/1>.
18. S. A. Maier, S. R. Andrews, L. Martín-Moreno, and F. J. García-Vidal, "Terahertz Surface Plasmon-Polariton Propagation and Focusing on Periodically Corrugated Metal Wires," *Phys. Rev. Lett.* **97**, 176805-1–4 (2006). URL <http://link.aps.org/abstract/PRL/v97/e176805>.
19. Y. Chen, Z. Song, Y. Li, M. Hu, Q. Xing, Z. Zhang, L. Chai, and C.-Y. Wang, "Effective surface plasmon polaritons on the metal wire with arrays of subwavelength grooves," *Opt. Express* **14**, 13,021–13,029 (2006). URL <http://www.opticsinfobase.org/abstract.cfm?URI=oe-14-26-13021>.
20. L. Shen, X. Chen, Y. Zhong, and K. Agarwal, "Effect of absorption on terahertz surface plasmon polaritons propagating along periodically corrugated metal wires," *Phys. Rev. B* **77**, 075408-1–7 (2008). URL <http://link.aps.org/abstract/PRB/v77/e075408>.
21. Q. Gan, Z. Fu, Y. J. Ding, and F. J. Bartoli, "Bidirectional subwavelength slit splitter for THz surface plasmons," *Opt. Express* **15**, 18,050–18,055 (2007). URL <http://www.opticsexpress.org/abstract.cfm?URI=oe-15-26-18050>.
22. Z. Ruan and M. Qiu, "Slow electromagnetic wave guided in subwavelength region along one-dimensional periodically structured metal surface," *Appl. Phys. Lett.* **90**, 201906-1–3 (2007). URL <http://link.aip.org/link/?APPLAB/90/201906/1>.
23. Q. Gan, Z. Fu, Y. J. Ding, and F. J. Bartoli, "Ultrawide-Bandwidth Slow-Light System Based on THz Plasmonic Graded Metallic Grating Structures," *Phys. Rev. Lett.* **100**, 256803-1–3 (2008). URL <http://link.aps.org/abstract/PRL/v100/e256803>.
24. S. S. Oh, S.-G. Lee, J.-E. Kim, and H. Y. Park, "Self-collimation phenomena of surface waves in structured perfect electric conductors and metal surfaces," *Opt. Express* **15**, 1205–1210 (2007). URL <http://www.opticsinfobase.org/abstract.cfm?uri=oe-15-3-1205>.
25. J. Shi, S.-C. Lin, and T. J. Huang, "Wide-band acoustic collimating by phononic crystal composites," *Appl. Phys. Lett.* **92**, 111901-1–3 (2008). URL <http://link.aip.org/link/?APPLAB/92/111901/1>.
26. Z. Ruan and M. Qiu, "Negative refraction and sub-wavelength imaging through surface waves on structured perfect conductor surfaces," *Opt. Express* **14**, 6172–6177 (2006). URL <http://www.opticsexpress.org/abstract.cfm?uri=oe-14-13-6172>.
27. S. A. Maier and S. R. Andrews, "Terahertz pulse propagation using plasmon-polariton-like surface modes on structured conductive surfaces," *Appl. Phys. Lett.* **88**, 251120-1–4 (2006). URL <http://link.aip.org/link/?APL/88/251120/1>.
28. C. Gómez-Reino, M. V. Perez, and C. Bao, *Gradient-index Optics: Fundamentals and Applications* (Springer, 2002).
29. D. T. Moore, "Gradient-index optics: a review," *Appl. Opt.* **19**, 1035–1038 (1980). URL <http://www.opticsinfobase.org/abstract.cfm?URI=ao-19-7-1035>.
30. A. O. Pinchuk and G. C. Schatz, "Metamaterials with gradient negative index of refraction," *J. Opt. Soc. Am. A* **24**, A39–A44 (2007). URL <http://www.opticsinfobase.org/abstract.cfm?URI=josaa-24-10-A39>.
31. H. Kurt and D. S. Citrin, "Graded index photonic crystals," *Opt. Express* **15**, 1240–1253 (2007). URL <http://www.opticsexpress.org/abstract.cfm?uri=oe-15-3-1240>.
32. P. Stellan, K. Tian, and G. Barbastathis, "Design of Gradient Index (GRIN) Lens using Photonic Non-Crystals," in *Conference on Lasers and Electro-Optics*, p. 1 (2007). URL <http://ieeexplore.ieee.org/search/wrapper.jsp?arnumber=4453288>.
33. F. S. Roux and I. D. Leon, "Planar photonic crystal gradient index lens, simulated with a finite difference time domain method," *Phys. Rev. B* **74**, 113103-1–4 (2006). URL <http://link.aps.org/abstract/PRB/v74/e113103>.

34. A. Taflove and S. Hagness, *Computational Electrodynamics: The Finite-Difference Time-Domain Method* (Artech House, Norwood, 2000).
35. V. A. Mandelshtam and H. S. Taylor, "Harmonic inversion of time signals and its applications," *J. Chem. Phys.* **107**, 6756–6769 (1997). URL <http://link.aip.org/link/?JCP/107/6756/1>.
36. A. Farjadpour, D. Roundy, A. Rodriguez, M. Ibanescu, P. Bermel, J. D. Joannopoulos, S. G. Johnson, and G. W. Burr, "Improving accuracy by subpixel smoothing in the finite-difference time domain," *Opt. Lett.* **31**, 2972–2974 (2006). URL <http://www.opticsinfobase.org/abstract.cfm?URI=ol-31-20-2972>.
37. J. Saxler, J. Gómez Rivas, C. Janke, H. Pellemans, P. Bolívar, and H. Kurz, "Time-domain measurements of surface plasmon polaritons in the terahertz frequency range," *Phys. Rev. B* **69**, 155,427-1–4 (2004). URL <http://link.aps.org/abstract/PRB/v69/e155427>.
38. W. Nomura, M. Ohtsu, and T. Yatsui, "Nanodot coupler with a surface plasmon polariton condenser for optical far/near-field conversion," *Appl. Phys. Lett.* **86**, 181,108-1–3 (2005). URL <http://link.aip.org/link/?APL/86/181108/1>.
39. Q. Gan, B. Guo, G. Song, L. Chen, Z. Fu, Y. J. Ding, and F. J. Bartoli, "Plasmonic surface-wave splitter," *Appl. Phys. Lett.* **90**, 161,130-1–3 (2007). URL <http://link.aip.org/link/?APL/90/161130/1>.
40. F. Lopez-Tejiera, S. Rodrigo, L. Martin-Moreno, F. Garcia-Vidal, E. Devaux, T. Ebbesen, J. Krenn, I. Radko, S. Bozhevolnyi, M. Gonzalez, *et al.*, "Efficient unidirectional nanoslit couplers for surface plasmons," *Nat. Phys.* **3**, 324–328 (2007). URL <http://www.nature.com/nphys/journal/v3/n5/abs/nphys584.html>.
41. P. Berini, "Plasmon polariton waves guided by thin lossy metal films of finite width: bound modes of symmetric structures," *Phys. Rev. B* **61**, 10484–10503 (2000). URL <http://link.aps.org/doi/10.1103/PhysRevB.61.10484>.
42. B. K. Juluri, Y. B. Zheng, D. Ahmed, L. Jensen, and T. J. Huang, "Effects of geometry and composition on charge-induced plasmonic shifts in gold nanoparticles," *J. Phys. Chem. C* **112**, 7309–7312 (2008). URL <http://dx.doi.org/10.1021/jp077346h>.

1. Introduction

Extraordinary optical transmission (EOT) is the enhanced transmission of incident electromagnetic radiation through sub-wavelength-scale holes in metallic films. [1, 2] EOT in real metals is based on two types of surface waves: 1) conventional surface plasmons (SPs) that are excited at a metal-dielectric interface, and 2) surface-bound states that exist on structured perfect electric conductor (PEC) surfaces. Although a PEC generally does not support any surface-bound states since an electromagnetic field cannot penetrate the surface, highly localized surface-bound states appear when the PEC is periodically modulated with arrays of sub-wavelength square or circular holes. Both theoretical [3, 4, 5, 6] and experimental [7, 8, 9, 10] studies suggest that surface-bound states and SPs exhibit similar dispersion relationships. Due to the similarity such surface-bound states are referred to as ‘spoof’ or ‘designer’ surface plasmons (DSPs).

Structured PEC surfaces and the excited DSPs have recently garnered interest within the photonics community, as a new platform to engineer surface-bound states of a wide frequency range. [11, 12, 13, 14] An important example is the guiding of terahertz-range radiation [15, 16] in the form of DSPs. This enables the application of terahertz plasmonics [17] to near-field imaging, sensing, and spectroscopy. A prime advantage of DSP is that, unlike conventional SP, the propagation of these waves can be controlled by engineering the material-independent, perceived group index. [3] PEC structures have been engineered to guide DSPs of specific terahertz-range frequencies. For example, periodically corrugated metal wires have been developed for guiding and focusing terahertz-frequency pulses [18, 19, 20]. By placing two optimized metallic grating structures on opposite sides of a narrow slit, Gan *et al.* were able to selectively guide terahertz-range waves along the two desired directions. [21] Similarly, metallic gratings have been found to significantly decrease the group velocity near the cutoff frequency. [22] Gan *et al.* [23] extended this notion by using graded metallic gratings to slow the propagation of wide-bandwidth, terahertz-range DSPs.

Successful applications of the propagation of DSPs on planar structures include waveguiding, imaging and sensing. Such applications require both vertical and lateral confinement of DSPs. To realize the latter, Oh *et al.* [24] exploited the anisotropic variation of the effective group indices of DSPs with frequency to achieve self-collimation [25]. Ruan *et al.* [26] achieved focusing/imaging by negative refraction. These methods work only at wavelengths comparable to the periodic spacing of the apertures

where the isofrequencies have zero or negative curvature. Another approach to realize lateral confinement was proposed by Maier *et al.*, in which a defect mode was realized by gradually increasing the hole size, leading to evanescent decay along the lateral direction. [27]

In this study, we demonstrate the lateral confinement of DSPs by engineering planar PEC structures as parabolic graded media. A lens with a parabolic gradient in its refractive index, N , transverse to the propagation of incident light, will cause the beam to propagate in a periodic fashion, as illustrated in Fig. 1(a). [28, 29] The parabolic gradient forces the beam to propagate periodically and can be explained by Snell's law. Electromagnetic energy emanating from a line source is focused in the first quarter pitch and later expanded/collimated in the second quarter pitch of the lens (the opposite is true for a point source). A similar effect has been observed for bulk waves in graded metamaterials of negative refractive indices [30] as well as for photonic crystals [31, 32, 33]. However, to-date no one has reported the propagation of surface waves like DSPs for perfect electric conductors using parabolic gradient index media. Such engineered structures would enable lateral confinement of DSPs at frequencies in the isotropic dispersion region, and would function as on-chip optical devices after the DSPs were excited and being guided.

To establish such a parabolic gradient in the effective group index along the direction transverse to the propagation of DSPs, we modulated either the size of the holes a or the dielectric constant ϵ_h of holes in the PEC structure, as shown in Fig. 1(b)-(c). Using a three-dimensional (3D) finite-difference time-domain (FDTD) method, we confirmed the effect of the parabolic gradient on the propagation of DSPs by achieving focusing, collimation, and wave-guiding (depending on the width of the light source). Our FDTD simulations agreed with analytic models from standard Gaussian optics.

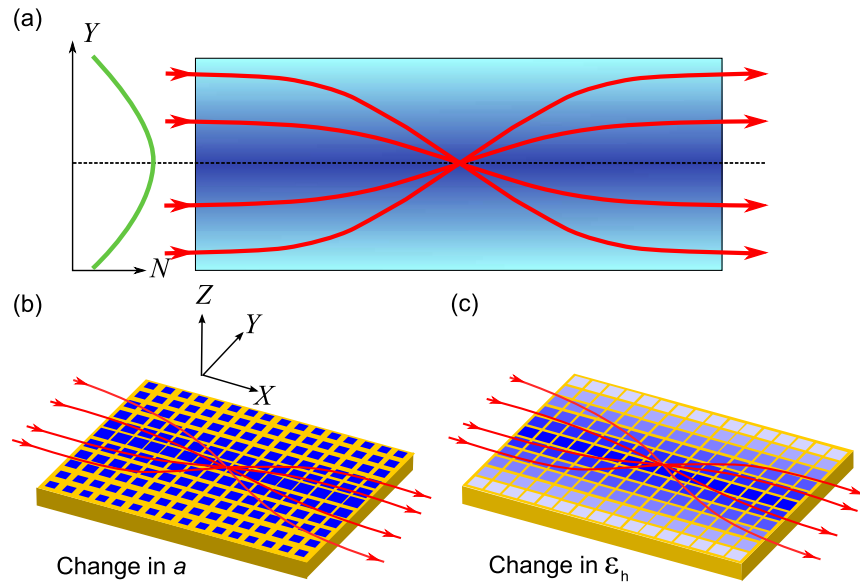


Fig. 1. (a) Principle of a gradient index based lens. A parabolic gradient (green line) of the group index (N) along the transverse direction of the propagation (Y -axis) enables the focusing or collimation of incoming beam (red arrows). A PEC structure with periodic array of square holes with varying (b) size of square holes and (c) dielectric constant, along the transverse direction of propagation (Y -axis) enables the focusing or collimation of DSPs (red arrows).

2. Design of the PEC structure

For a PEC structure with arrays of square holes having a lattice constant d , hole depth h , hole size a , and a dielectric constant ϵ_h , one can approximate the isotropic dispersion relation where $\lambda \gg d > a$, as [4]:

$$\frac{\sqrt{k_x^2 - k_o^2}}{k_o} = \frac{S^2 k_o}{\sqrt{\pi^2/a^2 - \epsilon_h k_o^2}} \left(\frac{1 - e^{-2|q_z|h}}{1 + e^{-2|q_z|h}} \right), \quad (1)$$

where k_x is the propagation constant, $k_o = \omega/c$, $S = 2a\sqrt{2}/\pi d$, and $q_z = i\sqrt{\pi^2/a^2 - \epsilon_h k_o^2}$. Using this equation one can solve for ω and differentiate with respect to k_x to obtain an expression for the effective group index:

$$N_g = \frac{c}{d\omega/dk_x} = \frac{\omega}{ck_x} \left[1 + \frac{2A\omega^2}{(\omega_{pl}^2 - \omega^2)} + \frac{A\omega^4}{(\omega_{pl}^2 - \omega^2)^2} - \frac{4A\sqrt{\epsilon_h}h\omega^4}{(\omega_{pl}^2 - \omega^2)^{3/2}} \left(\frac{e^{-2h|q_z|}}{1 - e^{-4h|q_z|}} \right) \right], \quad (2)$$

where ω_{pl} is the cutoff frequency such that $\omega_{pl} = \pi c/\sqrt{\epsilon_h}a$. A is given by

$$A = \frac{64a^4}{\pi^4 d^4 \epsilon_h} \left(\frac{1 - e^{-2|q_z|h}}{1 + e^{-2|q_z|h}} \right)^2. \quad (3)$$

Figure 2 shows the dispersion relations for various ϵ_h and a calculated per Eq. 1. The frequency and the wavevectors are presented in normalized units of $\frac{\omega d}{2\pi c}$ and $\frac{k_x d}{2\pi}$, respectively. An increase in a or ϵ_h will lead to a decrease in the cutoff frequency, ω_{pl} , thus decreasing the range of propagating modes. In order to realize periodic focusing of DSPs, the effective group index encountered by the DSPs should be parabolically modulated in the transverse direction. In principle, a change in either a , h or ϵ_h can be used to engineer the parabolic variation of N_g . For the application of this concept in the terahertz range, where a is in the range of 100's of μm , structured PEC material can be achieved by patterning a polymer using standard lithography and then electroplating the PEC material. Changes in a and h within PEC structures can be achieved by controlling the polymer pattern and time of electroplating, respectively. To control the dielectric constants, various refractive index oils can be filled into different holes using a precision fluid dispensing system coupled to a micro-positioner. However, resolving the small changes in a or h in a three-dimensional FDTD simulations is computationally challenging; we therefore focused our investigation on changing ϵ_h . Because both types of PEC structures can be fabricated and have similar behavior (as confirmed from the dispersion curves shown in Fig. 2), we believe that knowledge obtained from one structure can be applied to the other. Although one could calculate the dispersion relationships for various ϵ_h using Eq. 1, a mismatch at wavelengths comparable to the feature size is expected since the expression was derived for feature sizes much smaller than the wavelength of light. [6] Therefore, to obtain a more-accurate dispersion relation and modulation of ϵ_h with parabolic variation in N_g , we used a 3D FDTD method [34] to solve Maxwell's equations for homogeneous structures of different ϵ_h .

The dispersion relations were obtained by considering a single unit cell, as shown in the inset of Fig. 3(a), with Bloch periodic boundary conditions in the X and Y directions and perfectly matching layers (PMLs) along the Z direction. A grid size of $\delta x = \delta y = \delta z = d/15$ was used in the calculations. Excitation was achieved with a wide-band Gaussian source arbitrarily placed within the unit cell. Harmonic inversion of time signals [35] was used to extract the resonance modes for different ϵ_h with fixed d , $a = 0.85d$, and $h = 1.2d$. The FDTD calculations were performed using the open software package MEEP, wherein sub-pixel smoothing was used for increased accuracy. [36]

Figure 3(a) shows the dispersion relations calculated for different ϵ_h ranging from 1.25 to 3 in increments of 0.25. Keeping in view the practical importance of the proposed work in THz plasmonics

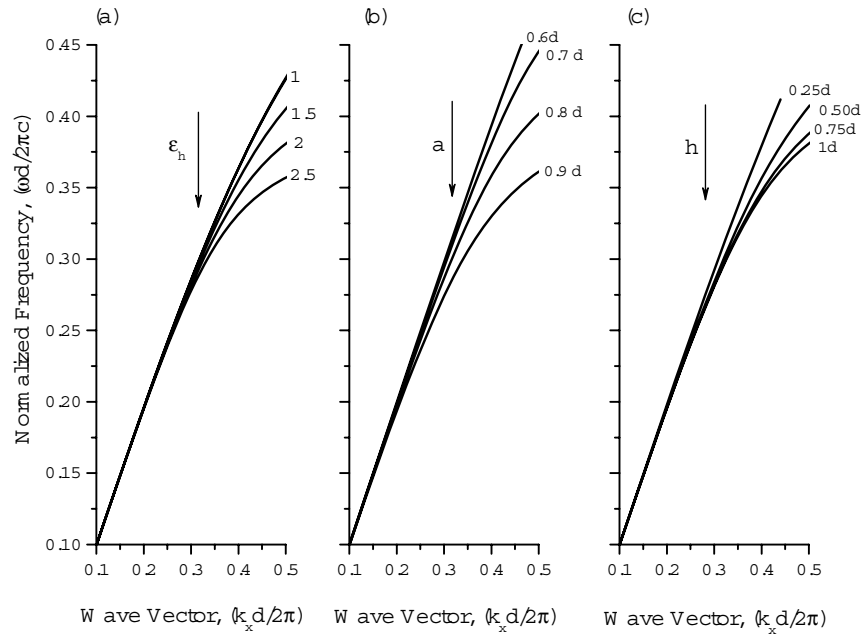


Fig. 2. Dispersion relations calculated using Eq. 1 for a PEC structure filled with (a) different ϵ_h and fixed $a=0.85d$, $h=1d$ (b) different a and fixed $\epsilon_h=2$, $h=1d$ and (c) different h with fixed $a=0.85d$, $\epsilon_h=2$.

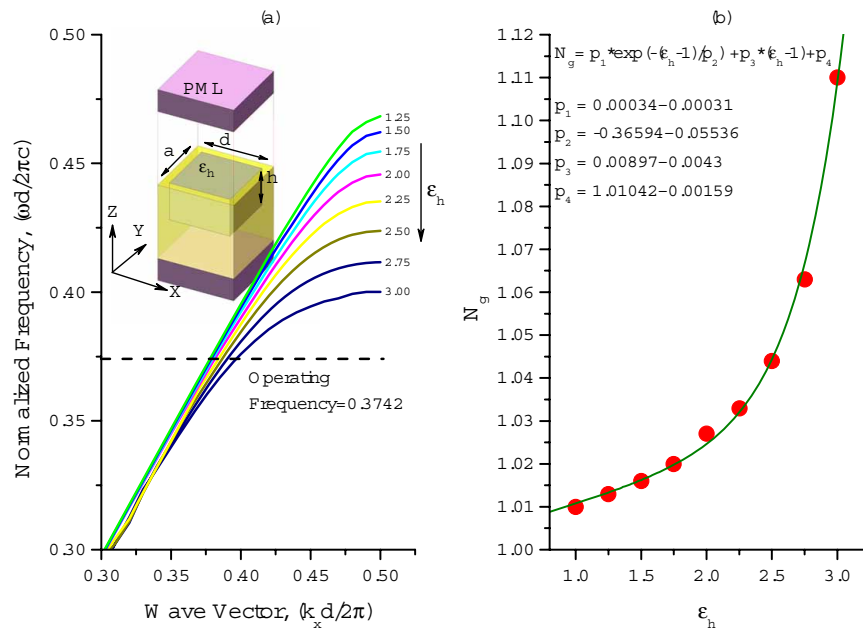


Fig. 3. (a) Dispersion relations calculated using FDTD for a PEC structure filled with different ϵ_h . Inset shows the unit cell. (b) Variation of N_g with ϵ_h at an operating frequency of 0.3742 normalized units obtained from FDTD (dotted line) and a best fit to the data (solid line).

research, we used an operating frequency of 1.122 THz, which for a hole depth of $d = 100\mu m$ yields an operating frequency of 0.3742 normalized units. For this operating frequency, the variation of N_g with respect to different ϵ_h was obtained by numerical differentiation and is shown in Fig. 3(b). The variation of N_g can be approximated with an exponential increase, as shown by the best fit (solid line) to the data points obtained by FDTD (dotted line).

Having established the relationship between N_g and ϵ_h at a certain operating frequency, we proceeded to design the graded index media and simulate via FDTD the propagation of designer plasmons. The 3D model used for FDTD consisted of a rectangular box of size $83d \times 23d \times 7d$ which included a PML thickness of $1d$ in each dimension, as shown in Fig. 4(a)-(c). To achieve 2D focusing and collimation of surface waves in the X-Y plane, we chose an effective group index that changed parabolically along the transverse direction of the propagation. The effective group index was highest at the center ($Y=0$) and varied along the positive and negative Y direction ($-10d$ to $10d$) as:

$$N_g^2(Y) = N_o^2[1 - (\alpha Y)^2] \quad (4)$$

where N_o is the group index at $Y = 0$ and α is the gradient coefficient. By choosing $N_o=1.1077$ and $N_g=1.014$ at $Y = \pm 10d$, we obtained a gradient with $\alpha=0.04031$. The variation of N_g with these parameters is shown in Fig. 4(d). To realize this group index change, the dielectric constant of the holes in the PEC-structured surface was altered by changing ϵ_h (based on a nearly exponential relationship between N_g and ϵ_h). The group index change is shown in Fig. 3(b). The exact distribution of ϵ_h along the transverse direction is shown in Fig. 4(d).

3. Results and discussion

The propagation of Gaussian beams with different beam widths in free-space parabolic graded lens was thoroughly studied by Gomez-Reino *et al.* [28] It has been shown that Gaussian beams with smaller beam widths expand and collimate in the first quarter pitch of the lens. Similarly, a Gaussian beam with a larger beam width gets focused and the beam width is decreased. At a certain beam width, when collimation and focusing effects cancel each other out, light will propagate at the same beam width through the structure. Our investigations focused on extending this physical mechanism from free-space optics to surface plasmons.

To investigate the efficiency of the proposed structure for lateral confinement of DSPs, we simulated the propagation of several DSPs that initiated from Gaussian beams of different beam widths relative to the lattice constant d . The use of Gaussian beams is appropriate in the context of THz plasmonics, since surface modes are excited on planar structures using Gaussian beams incident upon razor-blade-like structures. [37]

In simulation, the PEC was represented using a negative infinite dielectric constant and a grid size of $\delta x=\delta y=\delta z =d/15$ was used. The negative infinite dielectric constant creates the same effect as infinite conductivity by maintaining the electric field in the PEC structure at a constant value (zero in this case) Narrow-bandwidth TM-polarized (E_x , H_y , and E_z) Gaussian beams of different beam widths w at the operating frequency were launched in the X direction from $X=-40d$.

We first investigated the propagation of DSPs produced by a Gaussian beam of width $5d$ in a graded medium. As shown in Fig. 5(a)-(d), DSPs produced by such a wide source are focused as they reach $X=0$ (center of the structure) and then collimate after traveling $40d$. This result was expected that per Gaussian optics, electromagnetic energy in a material of parabolic graded index is guided in an oscillatory fashion with a periodic focal point. The X-Z view shows the localization of the E_z field along the surface of DSPs and also shows that the intensity increases at the center of the structure ($Y=0$) due to the focusing of the DSPs. This increase is seen in the snapshots of E_z field in the Y-Z plane at $X=-40d$ (Fig. 5(c)) and at $X=0$ (Fig. 5(d)). To qualitatively display the focusing effect, profiles of $|E_z|$ along the transverse direction at $X=-40d$ (dotted lines) and at $X=0$ (solid lines) are shown in Fig. 5(e). Focusing is evident from the increase in the intensity of E_z at $Y=0$ and from the lateral

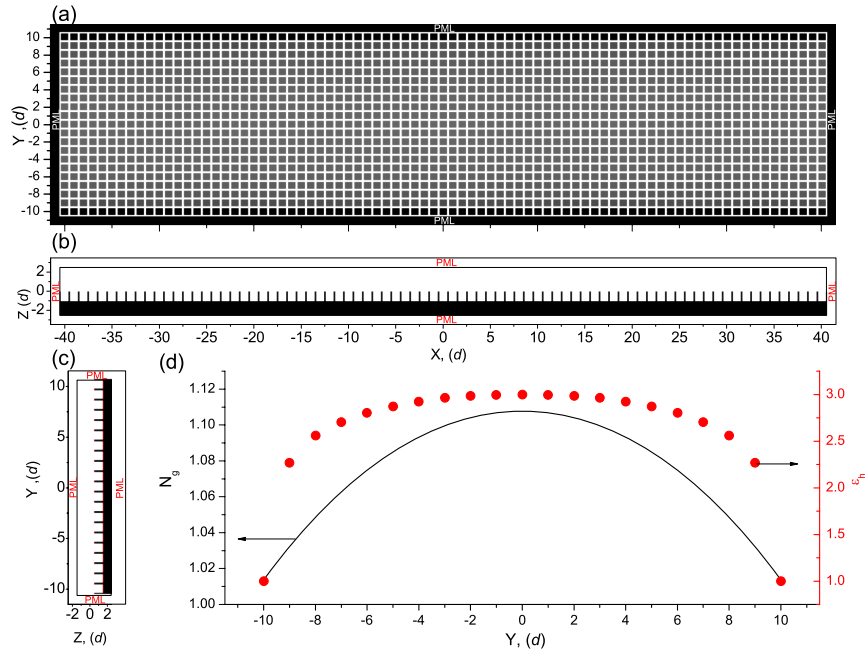


Fig. 4. FDTD model of graded PEC structure (a) X-Y view, (b) X-Z view, (c) Y-Z view, and (d) parabolic change of the N_g (line) and distribution of ϵ_h (dots) along the transverse direction of propagation (Y-axis) of DSPs. Perfect matching layers (PML) are employed at the boundaries of the simulation domain.

confinement. We also performed numerical simulations using similar source conditions and simulation geometries but with a uniform dielectric constant, and observed no focusing or collimation behavior (data not shown).

DSPs produced by Gaussian sources of smaller widths $w = 2d$ undergo collimation instead of focusing in the first half of the structure, and then focus in the second half of the structure (Fig. 6). From Fig. 6(e), we see that the collimation of DSPs in the first half of the structure results in a spreading of the intensity along the Y direction. In the absence of the graded media, the DSPs propagate radially (data not shown here).

With both Gaussian sources beam widths ($w = 5d$ or $2d$), DSPs either get collimated (Fig. 5) or focused (Fig. 6) by traveling a distance approximately $40d$. This distance matches closely with the quarter-pitch of graded lenses, $\frac{\pi}{2\alpha} = 39d$, predicted by standard Gaussian optics. At intermediate widths along the incident Gaussian beam, collimation and focusing cancel out [28]. DSPs are also guided along the length of the structure with no significant deviation in the beam width, as shown in Fig. 7 (a)-(e). This behavior allows one to guide energy in the form of DSPs over long distances.

Since many THz applications require that waveguides can squeeze electromagnetic waves into sub-wavelength areas, it is important to find out how tight the confinement of guided mode can be achieved using graded media and what parameters determine the tightness. We know from standard Gaussian optics for free-space graded lens that the minimum width of the beam in the graded lens is given by the fundamental mode, $w_{fm} = \sqrt{\frac{\lambda}{\pi N_o \alpha}}$ [28]. Based on the excellent match between the focusing lengths observed in our simulations and those observed in Gaussian optics, we infer that the confinement of spoof plasmons can be further improved by decreasing the wavelength or increasing the gradient or effective index at the center of the structure.

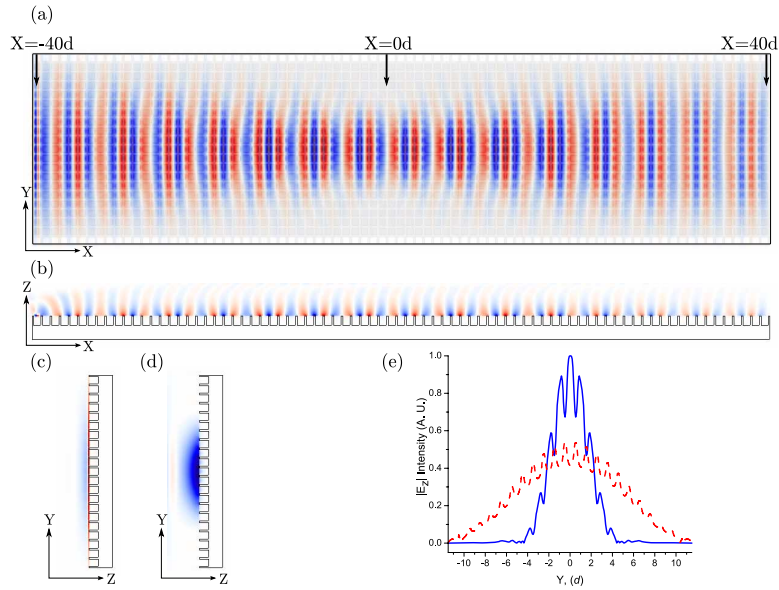


Fig. 5. Propagation of DSPs excited by Gaussian beams with $w = 5d$, snapshot of E_z field in a) $0.1d$ above X-Y plane b) X-Z plane, c) Y-Z plane at $X=-40d$ (source), d) Y-Z plane at $X=0d$ (midway) and e) comparison of the magnitude of E_z at $X=0d$ (solid line) and $X=-40d$ (dotted line).

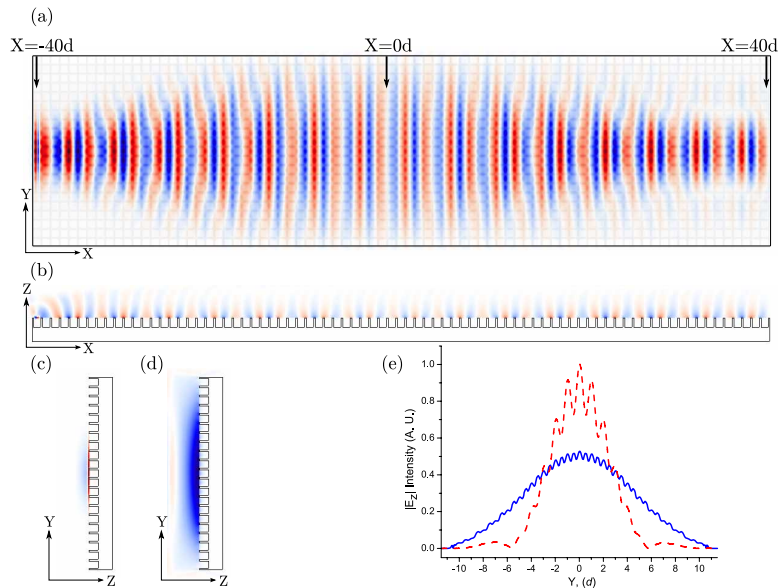


Fig. 6. Propagation of DSPs excited by Gaussian beams with $w = 2d$, snapshot of E_z field in a) $0.1d$ above X-Y plane b) X-Z plane, c) Y-Z plane at $X=-40d$ (source), d) Y-Z plane at $X=0d$ (midway) and e) comparison of the magnitude of E_z at $X=0d$ (solid line) and $X=-40d$ (dotted line).

Graded media can also be used to control the propagation of surface plasmons at visible and IR

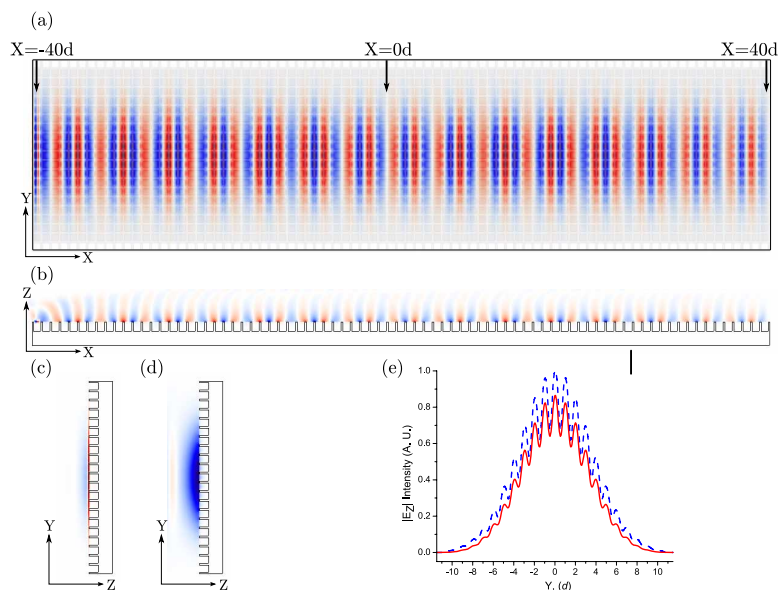


Fig. 7. Propagation of DSPs excited by Gaussian beams with $w = 3.5d$, snapshot of E_z field in a) $0.1d$ above X-Y plane b) X-Z plane, c) Y-Z plane at $X=-40d$ (source), d) Y-Z plane at $X=0d$ (midway) and e) comparison of the magnitude of E_z at $X=0d$ (solid line) and $X=-40d$ (dotted line).

domains using real metals. [38, 39, 40] Such an extension would require the consideration of absorption loss in real metals [41] due to dispersive nature [42] of real metals at visible frequencies. The effects of field penetration [24] in real metals should also be considered as it lowers the band positions observed in PEC structures.

4. Conclusions

Using FDTD simulations we have demonstrated that one can control the propagation of DSPs in structured PEC materials with arrays of square holes by exploiting graded index media. We found that graded index media can be realized by modulating either the size of the holes or the dielectric constant. Such a structure was engineered using FDTD simulations by modulating the dielectric constant of the structure's square holes and shown to provide lateral confinement of propagating DSPs. Focusing, collimation, and waveguiding of designer plasmons in a lateral direction were realized by changing the width of the source beam. These results will promote high confinement waveguide and sensing research for THz designer surface plasmons.

Acknowledgments

This research was supported by the National Science Foundation (ECCS-0824183 and ECCS-0801922), the Air Force Office of Scientific Research (AFOSR), the Penn State Center for Nanoscale Science (MRSEC), start-up funds from the Pennsylvania State University (PSU), and a seed grant from PSU's Research Computing and Cyberinfrastructure (a unit of Information Technology Services). The authors thank Jinjie Shi and Aitan Lawit for helpful discussions.